Acidity and Hydrophobicity of TS-1

Russell S. Drago,* Sílvia C. Dias,† J. Michael McGilvray, and Alfredo L. M. L. Mateus

Catalysis Center, Department of Chemistry, University of Florida, Gainesville, Florida 32611-7200

Received: October 6, 1997; In Final Form: November 17, 1997

This report investigates the causes of the unique properties and reactivity of the titanium silicalite TS-1, a commercial zeolite containing 1% Ti by weight. The combined analysis of calorimetric and adsorption data, cal−ad, for the reaction of TS-1 with pyridine shows the absence of the strong acid site found in HZSM-5 and the presence of only 0.07 mmol g^{-1} of a −15.1 kcal mol^{-1} hydrogen-bonding site. Titrations with 2,6-lutidine indicate the same number of hydrogen-bonding sites with a lower enthalpy (−9.8 kcal mol^{-1}). The magnitude of these enthalpies indicate that the acceptor sites are hydrogen-bonding sites that are comparable in acidity to the strongest sites on silica gel. The small amounts of these sites, 0.07 mmol g^{-1} compared to 0.8 mmol g^{-1} in silica gel and 0.5 mmol g^{-1} for the hydrogen-bonding sites of HZSM-5, account for the lower affinity of TS-1 for water. The absence of strong acidity prevents epoxide ring opening and explains the utility of TS-1 in epoxidation. Comparison of the results from the multiple equilibrium analysis of gas-phase adsorption isotherms for CO and CH_4 by TS-1, HZSM-5, and silica gel indicates that the surface of TS-1 is not more polarizable than the other solids. Thus, the porosity and small number of hydrogen-bonding-sites enables TS-1 to adsorb hydrocarbons in the presence of water.

Introduction

The ZSM-5 (MFI) zeolites are well-known for their excellent thermal as well as hydrothermal stability and find applications in acid-catalyzed hydrocarbon conversion reactions.[1] During the synthesis of TS-1, a titanium derivative of silicalite-1 (MFI structure) with a small fraction of isomorphous framework substitution of Si^{IV} by Ti^{IV}, the formation of a metallosilicate with no charge on the framework and thus no expected Brönsted acidity has been reported. X-ray powder diffraction indicates that TS-1 possesses the pentasil-type framework similar to that of HZSM-5.[3] An increase in unit-cell parameters with the degree of substitution and good agreement between the observed and calculated values of the Si−O and Ti−O distances support the isomorphous substitution of Si^{IV} by Ti^{IV}.[4] A BET surface area increase from 384 m^2 g^{-1} for silicalite ($Si_{96}O_{192}$) to 485 m^2 g^{-1} ($Si_{87.67}Ti_{8.33}O_{192}$) (Si/Ti = 10) is reported.[5]

There is a synthetic limit to the extent of isomorphous titanium substitution. Attempts to synthesize TS-1 with higher than 3% Ti content result in the formation of TiO_x nanophases.[6] When extraframework Ti^{IV} is present, the efficiencies of the catalysts in oxidation processes decrease drastically. Framework titanium in TS-1 is reported to give rise to a UV adsorption band at 210 nm. As the titanium content increases, the band broadens and shifts to that for TiO_2 (anatase) at 330 nm.

The catalytic properties of titanosilicalites are unique. In a variety of liquid-phase oxidation reactions of H_2O_2 with alcohols, ketones, alkanes, and cyclohexane, excellent selectivities results with only a slight loss of H_2O_2 from decomposition to H_2O and O_2.[7] Framework Ti^{IV} is indicated as the catalytic center because silicalite is catalytically inactive.[8] Differences in the reactivity of small and large alkenes and the reactivity of H_2O_2 and *t*-BuOOH oxidants indicate that the reaction takes place in the channels at titanium sites located in the framework.[6] Ti^{IV} in the framework positions (tetrahedral coordination) has low activity for H_2O_2 decomposition, and higher peroxide efficiencies are reported[8] with catalysts in which a separate TiO_2 phase is absent.

The active catalytic centers for oxidation are assigned to isolated, tetrahedral Ti^{IV} in an −Si−O−Ti−O−Si silica matrix that contains no Ti−O−Ti bonds. At room temperature, reversible hydrolysis of the Ti−O−Si bond takes place with the formation of Ti−OH and Si−OH groups. With H_2O_2, solvolysis produces TiOOH and SiOH with the former giving rise to the active catalytic oxidation center.[9]

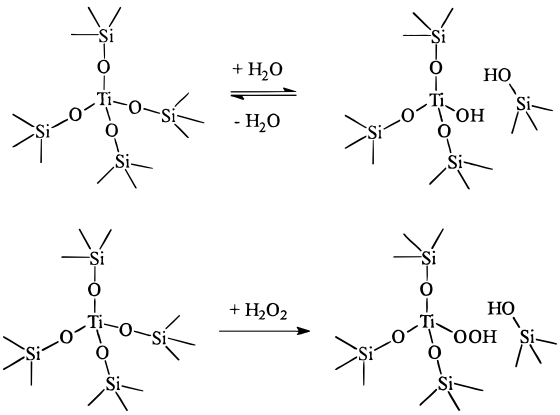

Oxidation of 1-hexene and *n*-octane with TS-1 occurs readily in aqueous or anhydrous solutions of H_2O_2. However, the same reaction with an amorphous, coprecipitated, TiO_2SiO_2 catalyst is inhibited when aqueous H_2O_2 is the oxidant.[10] TS-1 is reported[11] to be hydrophobic leading to the selective absorption of organic compounds from water solutions into the channels. This hydrophobicity is claimed to make TS-1 a highly efficient

* To whom correspondence should be addressed. Phone: (352) 392-6043. Fax: (352) 392-4658.

† Departamento de Química, Universidade de Brasília, Brasília-DF, 70919-910, Brazil.

S1089-5647(97)03249-5 CCC: $15.00
Published on Web 02/07/1998

TABLE 1: Summary of Gases and Physical Properties

probe gas	MW[a] (g/mol)	polarizability[b] (Å^3)	dipole moment (D)[c]	molar volume,[d] (mL/mol)	critical temperature (°C)	normal boiling point (°C)	ΔH_v (kcal/mol)	van der Waals const[a]	projected area [Å^2][d]
N_2	28.01	1.74	0	25.02	−146.9	−195.8	1.33	1.390	15.27
CO	28.01	1.95	0.13	28.28	−140.2	−191.5	1.44	1.485	15.77
CH_4	16.04	2.59	0	29.74	−82.60	−161.5	1.95	2.253	16.26
$(CH_3)_2O$	46.07	5.16	1.3	56.36	127	−25	36.78	8.073	26.16

[a] *Lange's Handbook of Chemistry*, 13th ed.; McGraw-Hill: NY, 1985. All data is from this source unless otherwise specified. [b] *Handbook of Chemistry and Physics*, 71st ed.; CRC Press: Florida, 1991. [c] McClellan, A. L. *Tables of Experimental Dipole Moments*; W. H. Freeman and Company: San Francisco, 1963; p 123. [d] Molar Volumes and cross-sectional areas calculated by ZINDO.[15d]

catalyst for oxidation of organic substrates using aqueous H_2O_2 as the oxidant.[11] TS-1 could be a more hydrophobic zeolite than HZSM-5 because its surface is more polarizable or because it contains less hydroxyl functionality. The hydrophobicity of TS-1 compared to silica could also result from a more polarizable surface or from microporosity in the former. An understanding of the reactivity of TS-1 requires an understanding of its acidity, the nature of its hydrophobicity, and the influence of its porosity on reactivity. To obtain this understanding, TS-1, HZSM-5, and silica gel have been selected for comparison.

We have previously described a cal−ad procedure for evaluating the acidity of silica gel,[12] HZSM-5,[13] and other solid acids.[14] This procedure employs the combined analysis of measurements from calorimetric and adsorption studies and provides the equilibrium constant ($K_{ads,i}$), the enthalpy ($-\Delta H_i$), and the number of acid sites (n_i) for each of the *i*-different types of sites in the solid. The solid is slurried in poorly solvating solvents to cancel nonspecific dispersion contributions and reactions with bases produce enthalpies that measure the donor−acceptor component. The multiple equilibrium analysis model[15a−c] probes porosity, surface polarity, and dispersion properties, as well as specific donor−acceptor interactions. This article reports measurement of adsorption thermodynamic parameters for TS-1 and determines how these properties account for the unique catalytic reactivity of TS-1.

Experimental Section

Materials. Calorimetric studies and infrared, liquid-, and gas-phase adsorption studies were performed on commercial samples of TS-1 containing 1% titanium by weight. Sample preparation consisted of drying the solid in flowing O_2 at 400 °C for 2 h followed by evacuation at 400 °C overnight. Elemental analysis performed by the Microanalysis Laboratory at the University of Florida revealed no carbon or nitrogen in the original and calcined samples.

Titanium was dispersed on silica (Davidson) by treatment with Ti(Oi-Pr)$_4$ under reflux in dry toluene, adapting a reported procedure.[16] This material was dried under vacuum at 140 °C overnight. $TiSiO_2$ has a titanium content of 1.5 wt % corresponding to the amount of Ti(Oi-Pr)$_4$ added.

The gases CO, CH_4, and $(CH_3)_2O$ (all 99.99%) were purchased from Matheson Gas Products and were used as received. Nitrogen (99.99%) was purchased from Liquid Air, Inc. Table 1 lists the physical properties of the gases studied. Pyridine (Fisher Scientific) was distilled over CaH_2 using a 12 in. Vigreux column and 2,6-lutidine (Aldrich, 97%) was used as supplied. Hexane (Aldrich, 99%) was distilled over P_2O_5 and stored over 4 Å molecular sieves.

Gas Adsorption Measurements. Adsorption measurements were performed on a Micromeretics ASAP 2000 instrument equipped with chemisorption/physisorption software employing a 47-point pressure table ranging from 0.1 to 760 Torr. The system was considered to be at equilibrium when the pressure change was less than 1% of the selected pressure point in a 10 s equilibration time interval. Low-temperature baths, consisting of a solvent/liquid nitrogen mixture, were used to collect isotherms at low temperatures. Temperatures above ambient were achieved by heating mantles which maintained the temperature to within ±1 °C. Sample loadings consisted of approximately 0.3 g of material. The adsorption data is obtained as unsmoothed data and is exported to a spreadsheet for further manipulation.

The adsorption data are fit to the MEA model (eq 1) where the total number of processes contributing to the adsorption isotherm is resolved.[15a]

$$[\mathrm{SA}]_s = \sum_i \frac{n_i K_i [P]}{1 + K_i [P]} \qquad (1)$$

Here [SA] is the total moles of adsorbate adsorbed per gram of solid, n_i is the capacity adsorbed for process *i* (mol/g), K_i is the equilibrium constant for process *i* (atm^{-1}), and *P* is the equilibrium pressure (atm). Use of this model to explain gas-phase adsorption processes of porous materials has been described elsewhere.[15]

Nitrogen porosimetry measurements at 77K were conducted to compare traditional surface areas and pore volumes with those from MEA. Surface areas were determined from a five-point BET calculation. Micropore volumes were determined from the Harkins−Jura *t*-plot model with thickness parameters from 5.5 to 10.0 Å. Macro- and mesopore volumes were calculated using the Barrett−Joyner−Halenda (BJH) desorption curve.

Catalyst Characterization. IR spectra were obtained from a Nicolet 5DXB FTIR spectrophotometer. Spectroscopic samples consisted of preparing a Nujol mull of the sample on NaCl plates under a dry nitrogen atmosphere. UV spectra of solids were obtained as Nujol mulls with a Perkin-Elmer Lambda 6 spectrophotometer. Epoxidation reactions were carried out in glass pressure bottles. Product analysis was done by GC using a HP 5890 Series II gas chromatograph equipped with a HP-50+ column. The products were verified with standards and quantification of the products was done using internal standards. Peroxide consumption was determined with iodometric titrations.

Cal−Ad Analysis of TS-1. Calorimetric and liquid adsorption measurements were performed on 1 g samples of TS-1. Both calorimetric and adsorption experiments involve slurrying the solid in a noncoordinating, poorly solvating solvent to minimize the solvent−solid and solvent−solute contributions. Hexane was chosen for this purpose because its molecular mass is comparable to pyridine.

For calorimetric experiments, known volumes of base solutions are added from a Hamilton 2.5 mL gastight syringe with calibrated stops. The heat evolved from each injection is

measured by a calibrated thermistor immersed in the slurried solution. Since the cal−ad analysis combines calorimetric and adsorption data from separate experiments, it is essential in the procedure to use the same ratio of solid to solution in both measurements.

For adsorption experiments, injections of known amounts of base are made to the slurried solvent which is stirred for approximately 3 min. A 1 mL sample of the solution is taken, and this sample is replaced with 1 mL of fresh solvent to maintain the proper solution-to-solid ratio. The equilibrium amount of free base in solution is measured with a Perkin-Elmer Lambda 6 UV−vis spectrophotometer in a 1 cm quartz cuvette at 251 nm for pyridine and at 265 nm for 2,6-lutidine. Calculation of the amount of base adsorbed onto the solid for each injection is given by the difference in the measured concentration of base in solution and the known concentration injected.

From the calculated values of base in solution and the amount adsorbed onto the solid, one can use an equation similar to eq 1 where the equilibrium pressure [*P*] is replaced by the equilibrium concentration of base in solution (mol/L).

$$[\mathrm{SA}] = \sum \frac{n_i K_i [\mathrm{B}]}{1 + K_i [\mathrm{B}]} \tag{2}$$

Multiple sites are required to fit the total adsorption isotherm to eq 2 enabling one to determine capacities n_i and equilibrium constants K_i for the resolvable adsorption sites. The resulting *K*'s and *n*'s are used to generate the equilibrium concentrations of base in solution that are too small to be measured by adsorption experiment. Rather than using a graphical interpolation of the adsorption isotherm to obtain these concentrations, the isotherm is fit to a polynomial.

For one site the following series is used:

$$(v/g)[\mathrm{T}] = x^2[\mathrm{B}]^2 + x[\mathrm{B}]$$

where v/g = volume (L)/mass of solid (g), [T] is the total concentration of base added (mol/L) for each injection in the calorimetric experiment, [B] is the equilibrium concentration of base in solution (mol/L), $x^2 = v/gK_1$ and $x = n_1K_1 - v/gK_1$-[T] + v/g.

For two sites the following series is used:

$$(v/g)[\mathrm{T}] = x^3[\mathrm{B}]^3 + x^2[\mathrm{B}]^2 + x[\mathrm{B}]$$

where $x^3 = K_1K_2\ v/g$, $x^2 = n_1K_1K_2 + n_2K_1K_2 - v/g_1K_2[\mathrm{T}] + v/gK_1 + v/gK_2$, and $x = n_1K_1 + n_2K_2 - v/gK_1[\mathrm{T}] - v/gK_2[\mathrm{T}] + v/g$.

The equilibrium concentrations for each base addition in the calorimetric experiment are calculated, and eq 3 is used to fit the calorimetric titration curve.

$$h/g = \sum \frac{n_i K_i [\mathrm{B}]}{1 + K_i [\mathrm{B}]} \Delta H_i \tag{3}$$

where *h*, the sum of heat evolved from calorimetric experiment, $= \Sigma\ ([\mathrm{T}] - [\mathrm{B}])\mathrm{v}\Delta H_i$ and ΔH_i is the enthalpy for binding to each site (kcal/mol); [T] is the total concentration of base added (mol/L) in each injection from calorimetric experiment; and [B] is the equilibrium concentration of base in solution (mol/L). In this manner the combined adsorption and calorimetric data are solved for the best fit *n*'s and *K*'s using a modified simplex fitting program.

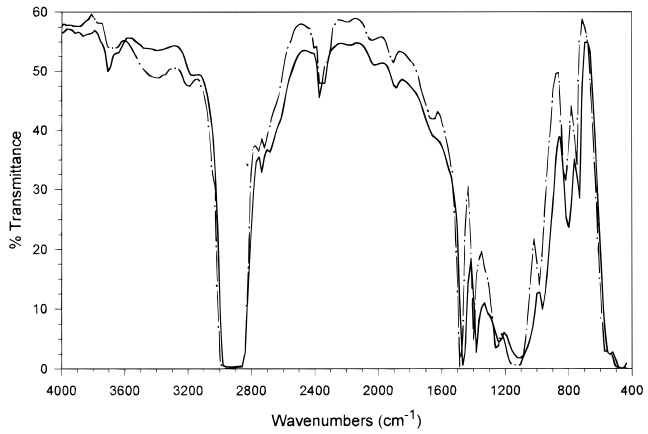

Figure 1. FTIR spectra in Nujol mulls of TS-1 as received (−•−) and after drying (—) at 400 °C in vacuum.

By iterating the calorimetric and adsorption data, one is able to optimize the n, K, and ΔH values for the individual *i* adsorption sites. Optimization is not considered to be complete until the values of K_i, n_i, and ΔH_i cease to change.

Results and Discussion

Sample Characterization. The synthesis of TS-1 is difficult to control, leading to variation in reactivity and selectivity for different samples.[8] Accordingly, effort was expended to characterize the sample used in this work. The infrared spectrum of our commercial TS-1 sample contains a broad adsorption band at 3400 cm^{-1} due to water and broad silanol bands around 3680 cm^{-1}, Figure 1. After drying for 24 h at 400 °C under vacuum, a sharp band remains at 3694 cm^{-1}. A band at the same frequency is present in HZSM-5 and is assigned to isolated silanol groups.[13] The peaks at 2900, 1460, 1377, and 730 cm^{-1} are from Nujol. When this sample is titrated with pyridine, the band at 3694 cm^{-1} disappears and two bands appear in the region (1800−1450 cm^{-1}) assigned to pyridine hydrogen-bond adducts (1600 and 1573 cm^{-1}). Peaks characteristic of the pyridinium ion were not observed confirming the absence of strong Brönsted acid sites in the TS-1 samples.

Titanium silicates exhibit an IR band at 960 cm^{-1}, assigned to the stretching mode of an [SiO_4] unit bonded to a tetrahedral Ti^{IV} ion or a titanyl group (>Ti═O), in the zeolite framework.[17,18] This band is not observed in the IR spectra of HZSM-5. Upon hydrogen bonding to pyridine, a shift of this Si−O−Ti stretching vibration to higher energy occurs. An additional band at ∼1100 cm^{-1} is assigned to asymmetric Si−O−Si network vibrations with the corresponding symmetric vibration at ∼800 cm^{-1}.

The UV spectrum of the TS-1 sample used in this study is shown in Figure 2, curve b, and is that assigned to an isolated Ti^{IV} charge-transfer transition[19] and it is in agreement with the literature.[18] To further verify the authenticity of our sample, the epoxidation of propylene was carried out using 30% aqueous H_2O_2 in CH_3CN solvent. Three atmospheres of propylene, 0.1 g of TS-1, 10 mmol of H_2O_2 and 10 mL of solvent led to 4.3 mmoles of propylene oxide in 2 h at room temperature. The peroxide consumed was 4.7 mmol corresponding to a 92% peroxide efficiency.

Equilibrium Gas Adsorption Analysis. Gaseous uptake measurements of CO, CH_4, and $(CH_3)_2O$ were performed on a commercial sample of TS-1 (1 wt % Ti) to afford a direct comparison of this solid with results reported for HZSM-5.[15c]

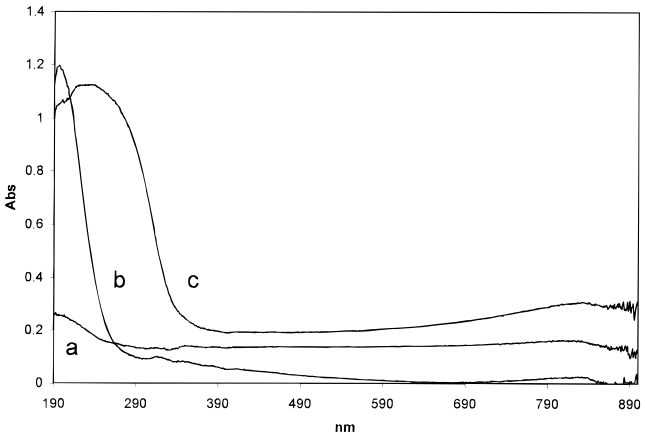

Figure 2. UV−vis spectra in Nujol mulls: (a) Silica Gel, (b) TS-1, (c) $TiSiO_2$.

TABLE 2: Temperature-Dependent Equilibrium Constants for TS-1 and HZSM-5[a]

temperature (°C)	K_1	K_2	K_3
	TS−1/CO		
−44	0.895 ± 0.006	0.125 ± 0.009	
−62	1.88 ± 0.009	0.257 ± 0.014	
−82	5.43 ± 0.02	0.653 ± 0.03	
	TS−1/CH_4		
−44	3.31 ± 0.01	0.093 ± 0.032	
−62	8.19 ± 0.05	0.3 ± 0.1	
−82	28.7 ± 0.3	0.96 ± 0.74	
	TS−1/$(CH_3)_2O$		
160	68 ± 31	3 ± 5	0. 5± 3
140	161 ± 18	5 ± 3	1 ± 2
125	276 ± 8	7 ± 1	1.4 ± 0.9
	HZSM−5/CO		
0	1.230 ± 0.004	0.182 ± 0.002	0.147 ± 0.003
−16	2.56 ± 0.07	0.454 ± 0.036	0.149 ± 0.041
−42	8.69 ± 0.67	1.48 ± 0.33	0.21 ± 0.38
−93	414 ± 6	28 ± 3	2.4 ± 3.2
	HZSM−5/CH_4		
0	1.279 ± 0.013	0.126 ± 0.028	
−16	2.309 ± 0.008	0.191 ± 0.018	
−42	8.14 ± 0.03	0.548 ± 0.066	
−84	85.8 ± 3.0	5.0 ± 6.7	
	HZSM−5/$(CH_3)_2O$		
200	713.4 ± 1.6	11.8 ± 6.4	0.39 ± 0.74
175	3731 ± 2.0	32.7 ± 8.0	0.83 ± 0.92
150	11546 ± 9.5	79 ± 37	1.5 ± 4.4

[a] In atm^{-1}.

The multiple temperature adsorption data are analyzed with the MEA model (eq 1) providing a measure of the free energy and enthalpy of binding as well as the process capacities. These afford measures of pore volumes and surface areas accessible to the adsorptive. For the adsorbates studied, the temperature-dependent equilibrium constants, $K_{i,ads}$ in atm^{-1} are given in Table 2. The corresponding enthalpies ($-\Delta H_i$, kcal mol^{-1}) for the processes are reported in Table 3 and the capacities n_i in mmol g^{-1} in Table 4. The enthalpies are determined from van't Hoff plots of the temperature-dependent equilibrium constants.

Adsorption of the unreactive, gaseous probe CH_4 characterizes the dispersion properties of the surface and gives information about the channel volumes and areas utilized by this non basic adsorptive. The MEA of methane adsorption by TS-1 requires two processes to describe the isotherm at the three temperatures near and above the critical temperature. The same number is required[15c] for HZSM-5 (bulk SiO_2/Al_2O_3 of 36 and a framework ratio of 50) which shares similar morphology. The magnitudes of the adsorption enthalpies for these two processes on both solids are those expected for physisorption and their similarity indicates that pores of comparable dimensions are involved. It is also of interest to note that Fisher silica gel has a small quantity of pores with enthalpies and thus dimensions comparable to the small pores of HZSM-5 and TS-1. The similarity of the methane adsorption enthalpies indicate that the surface of TS-1 is not more polarizable than HZSM-5 or silica gel.

TABLE 3: Thermodynamic Parameters Obtained in Gas Phase for Reaction of TS−1, HZSM-5, and Silica Gel with CO, CH_4, and $(CH_3)_2O$

adsorptive	process[a]	TS−1 $-\Delta H$	TS−1 $-\Delta S$	HZSM-5 $(-\Delta H)$	silica gel $(-\Delta H)$
CO	(1)			6.106 ± 0.088	
	1, (2)	4.1 ± 0.1	18.3	5.17 ± 0.28	4.1 ± 0.2
	2, (3)	3.8 ± 0.03	20.6	3.10 ± 0.48	3.6 ± 0.2
CH_4	1	4.9 ± 0.1	19.2	5.15 ± 0.13	4.6 ± 0.1
	2	5.3 ± 0.8	27.8	4.54 ± 0.1	3.2 ± 0.1
$(CH_3)_2O$	1	13.8 ± 0.9	23.4	22.0 ± 3.1	
	2	9.04 ± 1.4	17.0	15.0 ± 1.1	
	3	10.1 ± 1.9	24.8	10.4 ± 1.2	

[a] The process numbers in parentheses are labeled for CO adsorbed by HZSM-5. Process 2 for HZSM-5 should be compared to process 1 for TS-1 because strong acid sites are not present in the latter.

The n_i values in mmol g^{-1} are converted to capacities of the processes in mL/g^{-1} of solid using the molar volume. Contradictions in the literature molar volumes has prompted the use of molar volumes from molecular modeling of these adsorptives (Table 1).[15d] The resulting process volumes are given in Table 4. For methane, the small zigzag channels that lead to process one in HZSM-5 have twice the volume of the larger straight channels that lead to process 2. For methane adsorption by TS-1 there is slightly more volume in the smaller channels than in HZSM-5 and about the same volume of larger channels in the two solids. In silica gel, the quantity of small pores is very small and the process 2 capacity is 2−3 times larger than the large channel process 2 capacity of TS-1. The relative enthalpies indicate that silica gel uses larger pores in process 2 than TS-1 or HZSM-5. The total capacities indicate that, within experimental error, the total porosity used in methane adsorption above its critical temperature is the same for all three solids. The equilibrium pressures required to fill this capacity are larger for silica gel because the equilibrium constants are an order of magnitude smaller for the larger pores.[15c]

Adsorption of CO by TS-1 was best represented by a two process interpretation of the adsorption data. This result is in contrast to that of a three-process interpretation for CO adsorption by HZSM-5 and is similar to that of the two process adsorption by silica gel. The first process in HZSM-5 was attributed to a specific donor−acceptor interaction with very strong acid and hydrogen-bonding sites in the large and small channels.[15c] While the process enthalpies for CH_4 adsorption by TS-1 and HZSM-5 only differ by a few tenths of a kcal mol^{-1}, process 1 for CO on HZSM-5 is 2 kcal mol^{-1} larger than process 1 on TS-1. This indicates that the specific interactions leading to the strong acid and strong hydrogen-bonding sites of process 1 for CO in HZSM-5 are absent in TS-1. Processes 2 and 3 for HZSM-5, which correspond to small and large channel adsorption of CO, are comparable to processes 1 and 2 for TS-1. The process 2 adsorption enthalpy of CO in the small channel of HZSM-5 is larger than process 1 of TS-1. This 1 kcal mol^{-1} difference compared to that for

TABLE 4: Volumes and Surface Areas for TS-1, HZSM-5, and Silica Gel[a]

TS−1

	CO			CH_4			$(CH_3)_2O$		
process	mmol ads[b]	mL ads	area	mmol ads	mL ads	area	mmol ads	mL ads	area
n_1	2.17 ± 0.01	0.061	206.1	2.64 ± 0.02 0.01	0.0785	258.5	0.15 ± 0.04	0.0084	23.5
n_2	1.4 ± 0.08	0.040	133.0	0.99 ± 0.54	0.0294	96.9	0.9 ± 0.9	0.0495	137.6
n_3							1 ± 5	0.0701	203.3
total	3.57 ± 0.08	0.101	339.1	3.63 ± 0.54	0.1079	355.5	2 ± 5	0.1010	364.3

HZSM−5

	CO			CH_4			$(CH_3)_2O$		
process	mmol ads	mL ads	area	mmol ads	mL ads	area	mmol ads	mL ads	area
n_1	0.612 ± 0.028	0.0173	41.7	1.994 ± 0.044	0.0595	195.3	0.582 ± 0.005	0.033	91.7
n_2	1.22 ± 0.17	0.035	116.1	0.92 ± 0.68	0.0275	90.1	0.147 ± 0.067	0.007	23.2
n_3	1.08 ± 1.3	0.031	102.6				1.2 ± 2.7	0.068	189.1
total	2.9 ± 1.5	0.083	260.4	2.91 ± 0.72	0.0870	285.4	2.0 ± 2.8	0.109	303.9

Silica Gel

	CO			CH_4			propane		
process	mmol ads	ml ads	area	mmol ads	ml ads	area	mmol ads	ml ads	area
n_1	0.451 ± 0.002	0.0128	42.8	0.330 ± 0.001	0.0098	32.3	0.11 ± 0.0001	0.007	41.1
n_2	2.2 ± 0.1	0.062	209.0	3.03 ± 0.14	0.0901	296.7	2.8 ± 0.2	0.18	332.6
total	2.6 ± 0.1	0.075	251.8	3.3 ± 0.1	0.0999	329.0	2.9 ± 0.2	0.19	373.6

[a] Volumes in mL g^{-1}. Surface areas in m^2 g^1. [b] ads = adsorption.

methane (0.2 ± 0.2) suggests weak hydrogen bond sites contribute to the enthalpies for the small channel adsorption of CO in HZSM-5 (process 2). Within experimental error, the process 2 enthalpy for TS-1 is comparable to the process 3 enthalpy of HZSM-5 and both are attributed to adsorption in pores via nonspecific interactions. These results indicate that the acid hydroxyl functionality of HZSM-5 leads to specific interactions that cause the increased hydrophilicity of HZSM-5 compared to TS-1.

The TS-1 enthalpies are similar to those reported[15c] for CO adsorption by a commercial silica gel suggesting the absence of strong acid sites in the silica sample. The lower process 2 enthalpies for methane and comparable process 2 values for CO in TS-1 and silica gel suggests that small pores accessed by CO and not methane are included in the silica gel small pore size distribution. The silica gel process 1 volumes for CO and methane are consistent with this explanation.

To further probe acidic sites, gaseous dimethyl ether was studied as an adsorptive toward TS-1 and compared with HZSM-5. Adsorption of dimethyl ether by TS-1 was best described by a three-process interpretation of the adsorption data. The processes are readily distinguished at 125 °C by the *K* values. $(CH_3)_2O$ adsorption by HZSM-5 was also found to be best represented by a three-process interpretation of the adsorption data (Table 3). With this adsorbate, the interpretation of the processes is determined to a greater extent by the specific interactions than by pore dimensions. The difference in acidity is seen in a significant increase in the calculated enthalpy and equilibrium constant observed for the first process of HZSM-5 compared to TS-1 (enthalpies of −21 vs −14 kcal mol^{-1}). The magnitude of these enthalpies are indicative of a specific interaction and indicate a much weaker acidity for the strongest hydroxyl sites in TS-1 compared to HZSM-5. The process 2 enthalpy for HZSM-5 lies 3.9 kcal mol^{-1} above the van der Waals plot of process 1 enthalpies of poorly basic adsorbates on HZSM-5[15c] suggesting hydrogen bonding contributes to this process. Process 3 for HZSM-5 falls closely to the van der Waals plot and is mainly attributed to a dispersion interaction of dimethyl ether with the pore walls. The process 1 enthalpy for TS-1 indicates that this is a weak hydrogen bonding interaction. Process 2 and 3 enthalpies for TS-1 are attributed to dispersion interactions.

More information is provided by the capacities *n* reported in Table 4. With process 1 corresponding to the only specific interaction in TS-1, the small value of n_1 indicates that only a small amount, 0.15 mmol g^{-1}, of weak hydrogen-bonding sites exist. HZSM-5 has 0.71 mmol g^{-1} of specific sites in Process 1 and 2.

N_2 porosimetry measurements at 77 K resulted in a BET surface area of 470 m^2 g^{-1} for TS-1. Calculation of accessible surface areas are accomplished in MEA by converting n in mmol/g^{-1} to area using the projected area from molecular modeling of the adsorbates oriented so as to undergo maximum dispersion interaction with the surface (Table 1).[15d] Table 4 lists the resulting calculated surface areas for CO and CH_4 with TS-1. The surface area from MEA for CH_4 (355 m^2 g^{-1}) is less than that from BET. The difference is attributed to an overestimate from filling channel intersections with N_2 in the BET measurement. This adsorption does not occur with methane above the critical temperature. The MEA accessible pore volume of TS-1 is 0.1 mL for CO, CH_4, and $(CH_3)_2O$. The calculated Harkins−Jura *t*-plot micropore volume is 0.18 mL. The discrepancy again emphasizes that MEA measures the porosity involved in gas adsorption above the critical temperature. The difference would suggest 0.08 mL g^{-1} volume for the channel intersections. The MEA methane pore volume and surface areas for HZSM-5 are slightly smaller than those for TS-1.

Cal−Ad Results. A cal−ad analysis[12] of a commercial sample of TS-1 containing 1% titanium by weight was carried out. This sample, like HZSM-5 reported earlier, was dried at 400 °C. Pyridine and 2,6-lutidine were selected as donors in order to avoid the amphoteric interaction encountered when protonic donors (e.g., NH_3) are studied. The pyridine and 2,6-lutidine adsorption isotherms for TS-1 are shown in Figure 3 where the millimoles of base adsorbed by 1 g of the solid slurried in 100 mL of hexane are plotted vs the equilibrium amount of base in solution. Figure 3 also gives the results for the calorimetric titration by plotting the sum of heat evolved *h*′

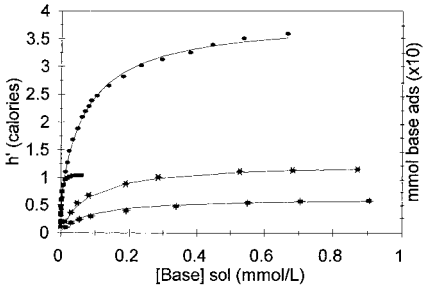

Figure 3. Adsorption isotherm and heat of adsorption versus concentration of base in solution. (shaded box) Calorimetric data points for pyridine. (dark circle) Adsorption data points for pyridine. (box with cross hairs) Calorimetric data points for 2,6-lutidine. (asterisk) Adsorption data points for 2,6-lutidine (multiplied by 2). (dash) Solid lines: calculated using values from Table 5.

versus moles of base added to 1 g of TS-1 slurried in 100 mL of hexane. The results of the cal−ad analysis of TS-1 are given in Table 5.

Comparison of the enthalpy of interaction of pyridine for the first site of TS-1 with that for HZSM-5[12] (−42 kcal mol^{-1}) shows that TS-1 does not have the very strong acid sites of HZSM-5 but is about as acidic as silica gel[11] conditioned at 200 °C (−12 kcal mol^{-1}). Thus TS-1, like silica gel, has only silanol hydrogen-bonding sites.[20] The *n*-values from cal−ad are particularly informative. Considering 1% titanium by weight, the sample has 0.23 mmol of Ti per gram and an empirical formula $Ti_{0.01}Si_{95.99}O_{192}$. The n_1 value of 0.07 mmol g^{-1} of hydrogen-bonding sites in TS-1 is much less than the amount of titanium and the 0.6 mol of acid sites (above 10 kcal mol^{-1}) in HZSM-5. A comparison of the pyridine cal−ad n_1 values for TS-1 (0.07 mmol) and silica gel evacuated at 200 °C (n_1 = 1.12 mmol) shows that silica gel also has a larger number of hydrogen-bonding sites than TS-1.

The titration of TS-1 with 2,6-lutidine gave a similar number of acid sites as pyridine. This indicates that vacant metal-centered Lewis sites do not exist. The lower enthalpy for 2,6-lutidine compared to pyridine suggests that some of the stronger hydrogen-bonding sites in the distribution are not accessed or ion pairing is less energetic with 2,6-lutidine. The two smallest dimensions of a molecule determine its ability to fit into a cylindrical channel. For pyridine and 2,6-lutidine, ZINDO calculations show[15d] these values are 3.3 × 6.5 and 4.1 × 7.0 Å, respectively. The adsorption isotherms of pyridine and 2,6-lutidine, shown in Figure 3, indicate that process 2 for pyridine is not near completion accounting for the large error in n_2 for pyridine on TS-1. The larger amount of pyridine adsorption observed for TS-1 is consistent with the sum of n_1 and n_2 for HZSM-5, which shows a significantly larger uptake of pyridine than 2,6-lutidine. The ratio of the molar volumes of 2,6-lutidine to pyridine is 1.4. Converting the moles adsorbed to volumes indicates that a 2:1 adsorbate volume ratio of pyridine to 2,6-lutidine occurs in HZSM-5. This ratio indicates limited access of 2,6-lutidine to the small pores of HZSM-5 as reported earlier[13] and suggests a similar restriction for TS-1.

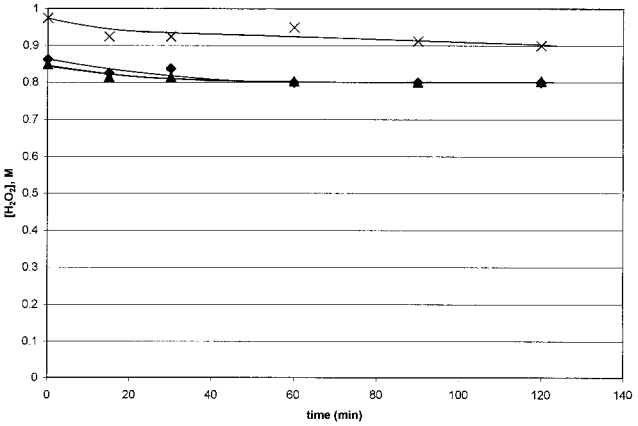

Figure 4. Hydrogen peroxide decomposition versus time at room temperature. (diamond) TS-1. (solid triangle) $TiSiO_2$. (times) TiO_2 (anatase).

Comparison of the area occupied by pyridine in process 1 (19.3 m^2 g^{-1}) with that for $(CH_3)_2O$ adsorption (23.5 m^2 g^{-1}) indicates that larger size of pyridine excludes access to some sites and in part accounts for the larger number of moles of $(CH_3)_2O$ involved in hydrogen bonding. Thus the cal−ad results, as well as MEA, indicate that the absence of acid sites in TS-1 leads to less capacity for water adsorption for TS-1 than HZSM-5 or silica and causes TS-1 to be less hydrophilic.

The pyridine second-site values for TS-1 are attributed to physisorption and the parameters are not well defined. Pyridine is competing with solvent for nonspecific adsorption. At the highest concentration employed to measure the adsorption isotherm, only 0.4 mmol of pyridine are added and this amount is insufficient to define the process parameters in the data analysis. Thus cal−ad and MEA are complimentary tools, with the former providing information about the donor acceptor interaction and the latter providing information about physisorption and specific interactions. When comparing the *n*'s or enthalpies from cal−ad to those from MEA, one should remember that cal−ad measures donor−acceptor interactions that are devoid of the dispersion component and MEA includes this contribution.[13]

Reactivity of TS-1 and Supported TiO_2. Differences in the reactivity and selectivity of TS-1 samples have been attributed to impurities in the catalyst. One way to probe the presence of impurities is to verify that the catalyst does not rapidly decompose hydrogen peroxide.[8] Impurities such as Fe^{3+}

TABLE 5: Thermodynamic Parameters Obtained in Hexane Solvent for Reaction of TS-1 with Pyridine and 2,6-Lutidine

	pyridine		lutidine	
	TS-1	HZSM-5[a]	TS-1	HZSM-5[a]
n_1 (mmol/g)	0.070 ± 0.005	0.042 ± 0.006	0.063 ± 0.004	0.053 ± 0.007
K_1 (M^{-1})	6.7 × 10^5 ± 2.2 × 10^4	4.9 × 10^6 ± 2.3 × 10^6	1.3 × 10^4 ± 3.7 × 10^2	7.4 × 10^5 ± 2.6 × 10^5
$-\Delta H_1$ (kcal/mol)	15.1 ± 0.4	42.1 ± 0.8	9.8 ± 0.5	19.0 ± 0.3
$-\Delta G_1$ (kcal/mol)	7.95	9.12	5.61	8.00
$-\Delta S_1$ (cal/deg)	24	111	14	37
n_2 (mmol/g)	0.31 ± 24	0.53 ± 0.01		0.13 ± 0.06
K_2 (M^{-1})	1.3 × 10^4 ± 1.1 × 10^5	2.3 × 10^4 ± 2.0 × 10^3		8.8 × 10^3 ± 2.3 × 10^3
$-\Delta H_2$ (kcal/mol)	0.02 ± 2.4	8.6 ± 3.8		5.4 ± 1.7
$-\Delta G_2$ (kcal/mol)	5.60	5.95		5.38
$-\Delta S_2$ (cal/deg)	−19	9		0.1

[a] Data from ref 13.

and Al^{3+}, introduced in the catalyst during the synthesis adversely affect hydrogen peroxide selectivities.[8] A 0.3 g sample of TS-1 was reacted with 1 mL of 35% H_2O_2 in 10 mL of CH_3CN. After 2 h at room temperature and at 40 °C, very little peroxide decomposition was observed. The same amounts of $TiSiO_2$ was reacted using the same conditions as in the TS-1 catalytic run. The results are shown in Figure 4. $TiSiO_2$ (1.5 wt % Ti) gave results very similar to TS-1. Bulk TiO_2 (anatase) also gave very little decomposition at these conditions. These results indicate that Ti(IV) is not an effective peroxide decomposition catalyst at 40 °C and raise questions concerning the role of extraframework titanium (TiO_2 phases) in peroxide decomposition at this temperature.

Conclusions

Measurements of adsorption isotherms for CO, CH_4, and $(CH_3)_2O$ as well as combined calorimetric titration and adsorption isotherm measurements (cal−ad) of the solid slurried in hexane reacting with pyridine are used to probe the cause of the hydrophobicity of TS-1. Multiple equilibrium analyses (MEA) indicate that the total pore volumes, surface areas, and surface polarizabilities are similar for HZSM-5, TS-1, and silica gel. Thermodynamic parameters for CH_4 adsorption are similar for HZSM-5 and TS-1, indicating similar porosity and a similar dispersion interaction with the solid surface. Both MEA and cal−ad show the absence in TS-1 of the very strong acid sites that are present in HZSM-5. The results also indicate a greatly reduced amount of hydrogen-bonding functionality on the interior and exterior surface of TS-1 compared to that of HZSM-5 or silica gel. The cal−ad method indicates that only 0.07 mmol per g^{-1} of hydrogen-bonding sites ($-\Delta H_1 = 15.1$ kcal mol^{-1}) exist on TS-1 compared to 0.6 mmol g^{-1} for HZSM-5. Thus, the absence of surface acidity (strong acid and hydrogen bonding), instead of an increased dispersion interaction, is the cause of the hydrophobic properties of TS-1 compared to those of HZSM-5.

Acknowledgment. Sílvia C. Dias and Alfredo L. M. L. Mateus are grateful to CNPq (Conselho Nacional de Desenvolvimento Científico e Tecnológico) for scholarship grants (proc. 200870/93-9 and 200053/96-5, respectively) to pursue a Ph.D. at the University of Florida. Sílvia C. Dias is also thankful to the Universidade de Brasília for the leave of absence during this period. The authors acknowledge the support of this research by the U.S. Army Research Office.

References and Notes

(1) Corma, A. *Chem. Rev. (Washington, D.C.)* **1995**, *95*, 559.

(2) Taramasso, M.; Perego, G.; Notari, B. U.S. Patent 4, 410, 501, 1983.

(3) Meier, W. M.; Olson, D. H. *Atlas of Zeolite Structure Types*; Butterworth-Heinemann: London, 1992; 138.

(4) Thangaraj, A.; Kumar, R.; Mirajkar, S. P.; Ratnasamy, P. *J. Catal.* **1991**, *130*, 1.

(5) Mirajkar, S. P.; Thangaraj, A.; Shiralkar, V. P. *J. Phys. Chem.* **1992**, *96*, 3073.

(6) Notari, B. *Catal. Today* **1993**, *18*, 163.

(7) Grzybowska-Swierkosz, B.; Haber, J. *Annu. Rep. Prog. Chem., Sect. C* **1994**, *91*, 403.

(8) Notari, B. *Adv. Catal.* **1996**, *41*, 253.

(9) Bellussi, G.; Carati, A.; Clerici, M. G.; Maddinelli, G.; Millini, R. *J. Catal.* **1992**, *133*, 220.

(10) Corma, A.; Esteve, P.; Martinez, A. *J. Catal.* **1996**, *161*, 11.

(11) Klein, S.; Maier, W. F. *Angew. Chem., Int. Ed. Engl.* 1996, *35*, 2230.

(12) Chronister, C. W.; Drago, R. S. *J. Am. Chem. Soc.* **1993**, *115*, 793.

(13) Drago, R. S.; Dias, S. C.; Torrealba, M.; Lima, L. *J. Am. Chem. Soc.* **1997**, *119*, 4444.

(14) Drago, R. S.; Kob, N. *J. Phys. Chem. B* **1997**, *101*, 3360.

(15) (a) Drago, R. S.; Burns, D. S.; Lafrenz, T. J. *J. Phys. Chem.* **1996**, *100*, 1718. (b) Drago, R. S.; Kassel, W. S.; Burns, D. S.; McGilvray, J. M.; Showalter, S. K.; Lafrenz, T. J. *J. Phys. Chem.* 1997. Accepted for publication. (c) Drago, R. S.; McGilvray, J. M.; Webster, C. E. 1997. Submitted for publication. (d) Webster, C.E.; Drago, R.S.; Zerner, M. 1997. Submitted for publication.

(16) Cativiela, C.; Fraile, J. M.; García, J. I.; Mayoral, J. A. *J. Mol. Catal. A* **1996**, *112*, 259.

(17) Szostak, R. *Handbook of Molecular Sieves*; von Nostrand Reinhold: New York, 1992.

(18) Clerici, M. G.; Ingallina, P.; Millini, R. *Proceedings of the 9th International Zeolite Conference*, Montreal, 1992; p 445.

(19) Klein, S.; Weckhuysen, B. M.; Martens, J. A.; Maier, W. F.; Jacobs, P. A. *J. Catal.* **1996**, *163*, 489.

(20) Clerici, M. G. *Appl. Catal.* **1991**, 68, 249.